Fermilab FERMILAB-Pub-02/054-E March 2002

Evidence for new interference phenomena in the decay $D^+ \to K^-\pi^+\mu^+\nu$

The FOCUS Collaboration ⋆

J. M. Link [a] M. Reyes [a] P. M. Yager [a] J. C. Anjos [b] I. Bediaga [b]
C. Göbel [b] J. Magnin [b] A. Massafferri [b] J. M. de Miranda [b]
I. M. Pepe [b] A. C. dos Reis [b] S. Carrillo [c] E. Casimiro [c]
E. Cuautle [c] A. Sánchez-Hernández [c] C. Uribe [c] F. Vázquez [c]
L. Agostino [d] L. Cinquini [d] J. P. Cumalat [d] B. O'Reilly [d]
J. E. Ramirez [d] I. Segoni [d] J. N. Butler [e] H. W. K. Cheung [e]
G. Chiodini [e] I. Gaines [e] P. H. Garbincius [e] L. A. Garren [e]
E. Gottschalk [e] P. H. Kasper [e] A. E. Kreymer [e] R. Kutschke [e]
L. Benussi [f] S. Bianco [f] F. L. Fabbri [f] A. Zallo [f] C. Cawlfield [g]
D. Y. Kim [g] A. Rahimi [g] J. Wiss [g] R. Gardner [h] A. Kryemadhi [h]
Y. S. Chung [i] J. S. Kang [i] B. R. Ko [i] J. W. Kwak [i] K. B. Lee [i]
K. Cho [j] H. Park [j] G. Alimonti [k] S. Barberis [k] M. Boschini [k]
P. D'Angelo [k] M. DiCorato [k] P. Dini [k] L. Edera [k] S. Erba [k]
M. Giammarchi [k] P. Inzani [k] F. Leveraro [k] S. Malvezzi [k]
D. Menasce [k] M. Mezzadri [k] L. Milazzo [k] L. Moroni [k] D. Pedrini [k]
C. Pontoglio [k] F. Prelz [k] M. Rovere [k] S. Sala [k]
T. F. Davenport III [ℓ] V. Arena [m] G. Boca [m] G. Bonomi [m]
G. Gianini [m] G. Liguori [m] M. M. Merlo [m] D. Pantea [m]
S. P. Ratti [m] C. Riccardi [m] P. Vitulo [m] H. Hernandez [n]
A. M. Lopez [n] H. Mendez [n] L. Mendez [n] E. Montiel [n] D. Olaya [n]
A. Paris [n] J. Quinones [n] C. Rivera [n] W. Xiong [n] Y. Zhang [n]
J. R. Wilson [o] T. Handler [p] R. Mitchell [p] D. Engh [q] M. Hosack [q]
W. E. Johns [q] M. Nehring [q] P. D. Sheldon [q] K. Stenson [q]
E. W. Vaandering [q] M. Webster [q] M. Sheaff [r]

[a] *University of California, Davis, CA 95616*
[b] *Centro Brasileiro de Pesquisas Físicas, Rio de Janeiro, RJ, Brasil*
[c] *CINVESTAV, 07000 México City, DF, Mexico*
[d] *University of Colorado, Boulder, CO 80309*
[e] *Fermi National Accelerator Laboratory, Batavia, IL 60510*

⋆ See http://www-focus.fnal.gov/authors.html for additional author information.

[f] *Laboratori Nazionali di Frascati dell'INFN, Frascati, Italy I-00044*
[g] *University of Illinois, Urbana-Champaign, IL 61801*
[h] *Indiana University, Bloomington, IN 47405*
[i] *Korea University, Seoul, Korea 136-701*
[j] *Kyungpook National University, Taegu, Korea 702-701*
[k] *INFN and University of Milano, Milano, Italy*
[ℓ] *University of North Carolina, Asheville, NC 28804*
[m] *Dipartimento di Fisica Nucleare e Teorica and INFN, Pavia, Italy*
[n] *University of Puerto Rico, Mayaguez, PR 00681*
[o] *University of South Carolina, Columbia, SC 29208*
[p] *University of Tennessee, Knoxville, TN 37996*
[q] *Vanderbilt University, Nashville, TN 37235*
[r] *University of Wisconsin, Madison, WI 53706*

Abstract

Using a large sample of charm semileptonic decays collected by the FOCUS photoproduction experiment at Fermilab, we present evidence for a small, even spin $K^-\pi^+$ amplitude that interferes with the dominant $\overline{K}^{*0}$ component in the $D^+ \to K^-\pi^+\mu^+\nu$ final state. Although this interference significantly distorts the $D^+ \to K^-\pi^+\mu^+\nu$ decay angular distributions, the new amplitude creates only a very small distortion to the observed kaon pion mass distribution when integrated over the other kinematic variables describing the decay. Our data can be described by $\overline{K}^{*0}$ interference with either a constant amplitude or broad spin zero resonance.

This paper describes discrepancies between the observed decay intensity for the decay $D^+ \to K^-\pi^+\mu^+\nu$ and that expected for pure $D^+ \to \overline{K}^{*0}\mu^+\nu$ decay. The data are overlayed with a simple model incorporating a particular choice of interference amplitude. A later paper will present the results of fits for the parameters describing the interfering amplitude along with new values of the form factors describing $D^+ \to \overline{K}^{*0}\mu^+\nu$.

Five kinematic variables that uniquely describe $D^+ \to K^-\pi^+\mu^+\nu$ decay are illustrated in Figure 1. These are the $K^-\pi^+$ invariant mass ($m_{K\pi}$) , the square of the $\mu\nu$ mass (q^2), and three decay angles: the angle between the π and the D direction in the $K^-\pi^+$ rest frame ($\theta_{\rm V}$), the angle between the ν and the D direction in the $\mu\nu$ rest frame (θ_ℓ), and the acoplanarity angle between the two decay planes (χ). The acoplanarity conventions for the D^+ and D^- will be discussed near the end of this paper.

It has been known for many years that the $D^+ \to K^-\pi^+\mu^+\nu$ final state is strongly dominated by the $D^+ \to \overline{K}^{*0}\mu^+\nu$ channel [1]. In the process of studying the $D^+ \to K^-\pi^+\mu^+\nu$ decay distribution, we found significant discrepancies between our data and the angular decay distributions for $D^+ \to \overline{K}^{*0}\mu^+\nu$ predicted using previously measured [2] form factor ratios. In particular, we discovered a significant forward-backward asymmetry in $\theta_{\rm V}$ suggesting a new term in the decay distribution that is linear in $\cos\theta_{\rm V}$ and a strong function of the kaon-pion mass. In pure $D^+ \to \overline{K}^{*0}\mu^+\nu$, the acoplanarity-averaged decay intensity should consist of terms with only even powers of $\cos\theta_{\rm V}$. In this paper we present an explicit model for this effect in terms of coherent interference between a small spin zero component of the kaon-pion system with a dominant $D^+ \to \overline{K}^{*0}\mu^+\nu$ component. Throughout this paper, we describe this interference as due to a constant, s-wave amplitude described by a single modulus and phase. We do not exclude the possibility of a broad spin zero resonance or even higher spin resonances with helicity amplitudes tuned to resemble the behavior of a single, broad s-wave resonance.

Angular momentum considerations allow us to predict the dependence of the interference-induced, linear $\cos\theta_{\rm V}$ term on other decay variables such as q^2, θ_ℓ , and χ. We present this model and show how well our data match these predictions. Throughout this paper, unless explicitly stated otherwise, the charge conjugate is also implied when a decay mode of a specific charge is stated.

The data for this paper were collected in the Wideband photoproduction experiment FOCUS during the Fermilab 1996–1997 fixed-target run. In FOCUS, a forward multi-particle spectrometer is used to measure the interactions of high energy photons on a segmented BeO target. The FOCUS detector is a large aperture, fixed-target spectrometer with excellent vertexing and particle identification. Most of the FOCUS experiment and analysis techniques have been described previously [3]. Here, for the first time, we describe our muon

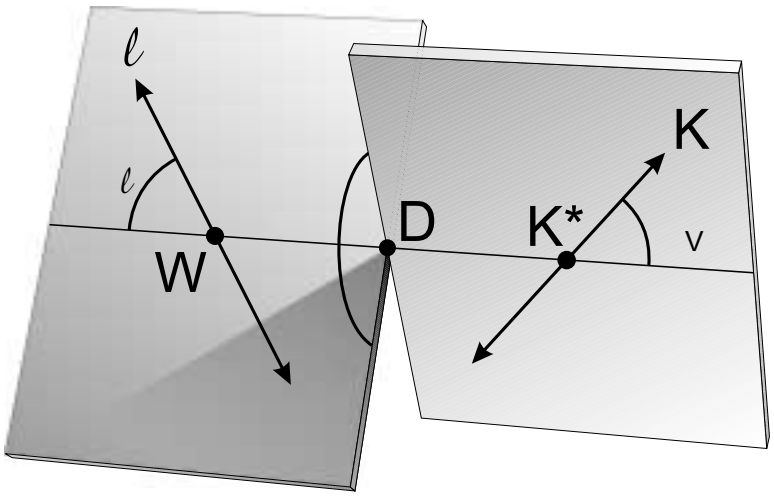

Fig. 1. Definition of kinematic variables.

identification. FOCUS uses two muon detector systems, the inner muon hodoscope, and the outer muon detector. Muons are identified by their ability to penetrate approximately 21 interaction lengths of absorber for the inner muon system, and 18 interaction lengths for the outer system. For the inner system, potential muon tracks are projected through the electromagnetic and hadronic calorimeters, and additional iron shielding walls. This trajectory is then matched to hits recorded in an inner muon detector consisting of six arrays of scintillation counters subtending approximately ± 45 mrad. The outer muon detector consists of three views of resistive plate chambers which are shielded by the outer electromagnetic calorimeter and the iron yoke of the second analysis magnet. This subtends an additional region of roughly ± 140 mrad. For the outer muon system, potential muon tracks are projected through the magnet yoke and then matched to outer muon hits.

Our analysis cuts were chosen to give reasonably uniform acceptance over the 5 kinematic decay variables, while still maintaining a reasonably strong rejection of backgrounds. To isolate the $D^+ \to K^-\pi^+\mu^+\nu$ topology, we required that candidate muon, pion, and kaon tracks appeared in a secondary vertex with a confidence level exceeding 5%. The muon track, when extrapolated to the shielded muon arrays, was required to match muon hits with a confidence level exceeding 5%. The kaon was required to have a Čerenkov light pattern more consistent with that for a kaon than that for a pion by 2 units of log likelihood, while the pion track was required to have a light pattern favoring the pion hypothesis over that for the kaon by 2 units [4].

To further reduce muon misidentification, an inner muon candidate was allowed to have at most one missing hit in the 6 planes comprising our inner muon system. In order to suppress muons from pions and kaons decaying in our spectrometer, we required inner muon candidates to have an energy exceeding 8 GeV. For outer muons we required an energy exceeding 6 GeV. Non-charm and random combinatoric backgrounds were reduced by requir-

ing both a detachment between the vertex containing the $K^-\pi^+\mu^+$ and the primary production vertex of 12 standard deviations and a minimum visible energy ($E_K + E_\pi + E_\mu$) of 30 GeV. To suppress possible backgrounds from higher multiplicity charm decay, we isolate the $K\pi\mu$ vertex from other tracks in the event (not including tracks in the primary vertex) by requiring that the maximum confidence level for another track to form a vertex with the candidate be less than 0.1%.

In order to allow for the missing energy of the neutrino in this semileptonic D^+ decay, we required the reconstructed $K\pi\mu$ mass be less than the nominal D^+ mass. Background from $D^+ \to K^-\pi^+\pi^+$, where a pion is misidentified as a muon, was reduced using a mass cut: we required that when these three tracks were reconstructed as a $K\pi\pi$, their $K\pi\pi$ invariant mass differed from the nominal D^+ mass by at least three standard deviations. In order to suppress background from $D^{*+} \to D^0\pi^+ \to (K^-\mu^+\nu)\pi^+$ we required $M(K^-\mu^+\nu\pi^+) - M(K^-\mu^+\nu) > 0.18$ GeV/c^2. The momentum of the undetected neutrino was estimated from the D^+ line-of-flight as discussed below.

We assumed that the reconstructed D momentum vector points along the direction defined by the primary and secondary vertices. This leaves a two-fold ambiguity on the neutrino momentum. We use the solution that gives the lower D momentum, which, according to our Monte Carlo studies, produced somewhat better estimates for the kinematic variables. Due to resolution, 50% of events were reconstructed outside physical limits (the $p_\perp$ of the charged daughters relative to the D^+ direction implied a parent mass larger than the nominal D^+ mass). These events are recovered by moving the primary vertex to the nearest allowed solution and the kinematic variables are recomputed. Monte Carlo studies show that the inclusion of the recovered events does not significantly degrade either the resolution or the signal-to-noise ratio.

It was important to test the fidelity of the simulation with respect to reproducing the resolution of those kinematic variables which depend on the neutrino momentum. To do this, we studied fully-reconstructed $D^0 \to K^-\pi^+\pi^+\pi^-$ decays where, as a test, one of the pions was reconstructed using our line-of-flight technique. We then compared its reconstructed momentum to its original, magnetic reconstruction in order to obtain an "observed" resolution function that was well matched by our simulation.

Figure 2 shows the $K^-\pi^+$ mass distribution for the signal we obtained using the cuts described above. A very strong $\overline{K}^{*0}(896)$ signal is present. To assess the level of non-charm backgrounds, we plot the "right-sign" (where the kaon and muon have the opposite charge) and "wrong-sign" $K^-\pi^+$ mass distributions separately. We subtract the distributions of wrong-sign from right-sign events as a means of subtracting non-charm backgrounds that are nearly charge symmetric.

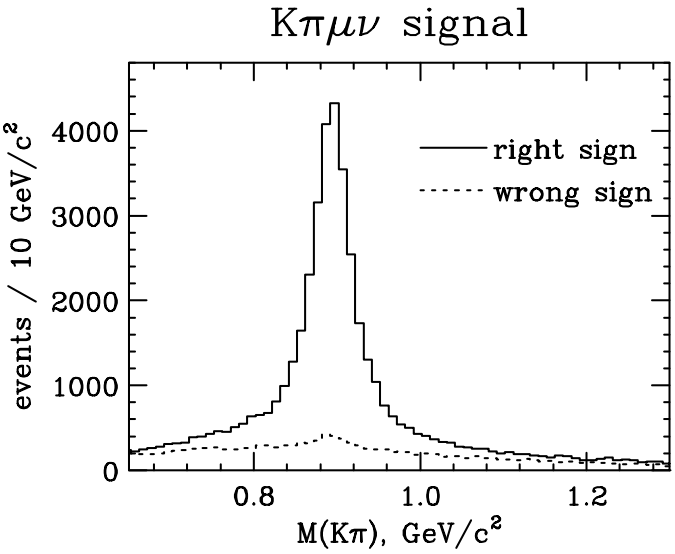

Fig. 2. $D^+ \to K^-\pi^+\mu^+\nu$ signal. Right-sign and wrong-sign samples are shown. The approximate wrong-sign-subtracted yield is 31 254 events. In the mass window from 0.8–1.0 GeV/c^2 there is a right-sign excess of 27 178 events. A Monte Carlo that simulates the production and decay of all known charm species predicts that ≈7% of this excess is actually background from other charm decays.

Figure 3 compares the wrong-sign-subtracted $\cos\theta_{\rm V}$ distribution to that predicted by our Monte Carlo which incorporates all acceptance, and resolution effects as well as all known charm backgrounds. We show separate distributions for events with a $K^-\pi^+$ mass in the range $0.8 < m_{K\pi} < 0.9\,{\rm GeV}/c^2$ and $0.9 < m_{K\pi} < 1.0\,{\rm GeV}/c^2$.

Although the events with a reconstructed mass above 0.9 GeV/c^2 are a reasonable match to the prediction, a striking discrepancy is apparent in the $\cos\theta_{\rm V}$ distribution for those events below the pole. As will be explained in detail later, we believe this can be explained by the interference of a broad (or nearly constant) s-wave amplitude with the Breit-Wigner amplitude describing the $\overline{K}^{*0}$. In particular, this interference creates a term in the decay intensity that, when averaged over acoplanarity, is linear in $\cos\theta_{\rm V}$ whereas the pure $D^+ \to \overline{K}^{*0}\mu^+\nu$ process produces only even powers in $\cos\theta_{\rm V}$ in this intensity. The slight forward-backward asymmetry present in the Monte Carlo histograms of Figure 3 primarily reflects acceptance variation. [1]

We exploit the fact that all acoplanarity-averaged terms in the decay intensity expected for pure $D^+ \to \overline{K}^{*0}\mu^+\nu$ should be proportional to even powers of $\cos\theta_{\rm V}$ (see Eqn. 1 below). Because our analysis cuts give reasonably uniform acceptance over $\cos\theta_{\rm V}$, we can construct a weight designed to project out any linear $\cos\theta_{\rm V}$ contribution to the decay distribution. This weight is the product

[1] The known charm backgrounds tend to have the opposite $\cos\theta_{\rm V}$ asymmetry to that observed in Figure 3. Their level can also be significantly reduced under tighter analysis cuts that still preserve the much larger asymmetry in the data.

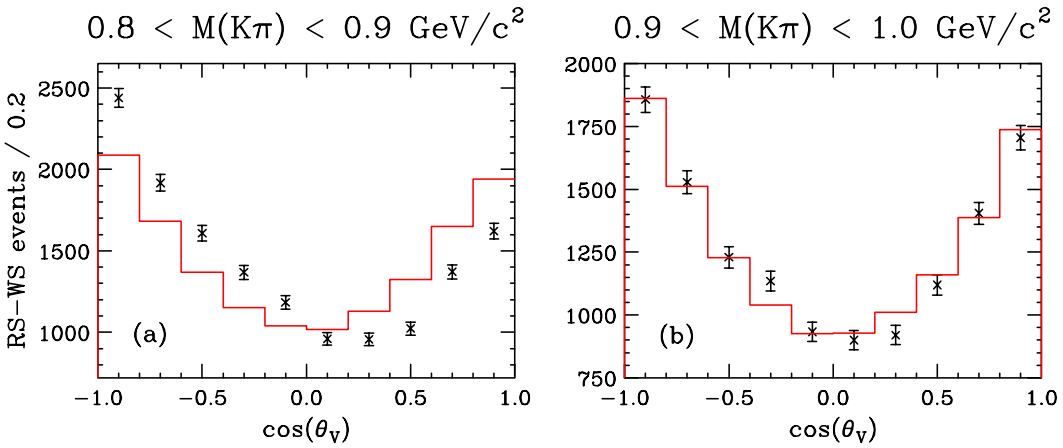

Fig. 3. Event distribution in $\cos\theta_{\rm V}$, split between samples above and below 0.9 GeV/c^2. The points with error bars are (wrong-sign subtracted) FOCUS data and the solid histogram is a Monte Carlo simulation, including the signal with the measured form factor ratios [2] and all known charm backgrounds. The Monte Carlo is normalized by area for each plot independently.

of a wrong-sign subtraction weight (+1 for right-sign and -1 for wrong-sign) multiplied by $\cos\theta_{\rm V}$. The weighted $m_{K\pi}$ distribution is shown in Figure 4 and compared to two Monte Carlo simulations. One Monte Carlo is based on pure $D^+ \to \overline{K}^{*0}\mu^+\nu$ and known charm backgrounds (dashed histogram) while the second (solid histogram) also includes the interfering s-wave amplitude that we will describe later. The dashed histogram shows that the residual effects of charm backgrounds, acceptance variation and resolution effects produce a much smaller variation with $\cos\theta_{\rm V}$ than we observe. The striking mass dependence of the linear $\cos\theta_{\rm V}$ term displayed in Figure 4 will be the principal tool we will use to estimate the parameters of the interfering amplitude. Figures 5–6 compare the dependence of the $\cos\theta_{\rm V}$ asymmetry on two other kinematic variables ($\cos\theta_\ell$ and q^2) to the Monte Carlo with and without the s-wave amplitude. The acoplanarity dependence of the interference term will be discussed in a later section.

It was possible to understand the forward-backward asymmetry in $\cos\theta_{\rm V}$ using a simple model summarized by Eqn. 1. Using the notation of [5], we write the decay distribution for $D^+ \to K^-\pi^+\mu^+\nu$ in terms of the three helicity basis form factors: H_+ , H_0 , H_-. For simplicity, we show the decay distribution in the limit of zero lepton mass

$$\frac{d^5\Gamma}{dm_{K\pi}\; dq^2\; d\cos\theta_{\rm V}\; d\cos\theta_\ell\; d\chi} \propto Kq^2 \left| \begin{array}{l} (1+\cos\theta_\ell)\sin\theta_{\rm V} e^{i\chi} {\rm B}_{K^{*0}} H_+ \\ -(1-\cos\theta_\ell)\sin\theta_{\rm V} e^{-i\chi} {\rm B}_{K^{*0}} H_- \\ -2\sin\theta_\ell(\cos\theta_{\rm V} {\rm B}_{K^{*0}} + Ae^{i\delta})H_0 \end{array} \right|^2 \quad (1)$$

where K is the momentum of the $K^-\pi^+$ system in the rest frame of the D^+. The helicity basis form factors are given by:

$$H_{\pm}(q^2) = (M_D + m_{K\pi})A_1(q^2) \mp 2\frac{M_D K}{M_D + m_{K\pi}}V(q^2)$$

$$H_0(q^2) = \frac{1}{2m_{K\pi}\sqrt{q^2}}\left[(M_D^2 - m_{K\pi}^2 - q^2)(M_D + m_{K\pi})A_1(q^2) - 4\frac{M_D^2 K^2}{M_D + m_{K\pi}}A_2(q^2)\right]$$

The vector and axial form factors are parameterized by a pole dominance form:

$$A_i(q^2) = \frac{A_i(0)}{1 - q^2/M_A^2} \qquad V(q^2) = \frac{V(0)}{1 - q^2/M_V^2}$$

where we use world average [2] values of $R_V \equiv V(0)/A_1(0) = 1.82$ and $\mathrm{R}_2 \equiv \mathrm{A}_2(0)/\mathrm{A}_1(0) = 0.78$ and nominal (spectroscopic) pole masses of $M_A = 2.5$ GeV/c^2 and $M_V = 2.1$ GeV/c^2. [2]

The $\mathrm{B}_{K^{*0}}$ stands for a Breit-Wigner amplitude (Eqn. 2) describing the $\overline{K}^{*0}$ resonance: [3]

$$\mathrm{B}_{K^{*0}} = \frac{\sqrt{m_0\Gamma}\left(\frac{P^*}{P_0^*}\right)^{(3/2)}}{m_{K\pi}^2 - m_0^2 + im_0\Gamma\left(\frac{P^*}{P_0^*}\right)^3} \tag{2}$$

In Eqn. 1, the s-wave amplitude is modeled as a constant (no variation with $m_{K\pi}$) with modulus A and phase δ. Angular momentum conservation restricts its contribution to the H_0 piece that describes the amplitude for having the virtual W^+ in a zero helicity state relative to its momentum vector in the D^+ rest-frame.

Assuming this new, previously unreported amplitude is small, it will primarily affect the decay distribution through interference with the dominant Breit-Wigner amplitude. Expanding Eqn. 1, we find that interference between the s-wave amplitude and the $\mathrm{B}_{K^{*0}}$ amplitude produces the following three interference terms:

[2] Eqn. 1 implicitly assumes that the q^2 dependence of the s-wave amplitude coupling to the virtual W^+ is the same as the H_0 form factor describing the $D^+ \to \overline{K}^{*0}\mu^+\nu$. This assumption is consistent with our data as illustrated in Figure 6. The modulus A would then be the form factor ratio.

[3] We are using a p-wave Breit-Wigner form with a width proportional to the cube of the kaon momentum in the kaon-pion rest frame (P^*) over the value of this momentum when the kaon-pion mass equals the resonant mass (P_0^*).

$$\text{Interfere} = 8\cos\theta_{\rm V}\sin^2\theta_\ell A\Re\left(e^{-i\delta}{\rm B}_{K^{*0}}\right)H_0^2 \qquad \text{(3-a)}$$

$$-\,4(1+\cos\theta_\ell)\sin\theta_\ell\sin\theta_{\rm V}\;A\Re\left(e^{i(\chi-\delta)}{\rm B}_{K^{*0}}\right)H_+H_0 \qquad \text{(3-b)}$$

$$+\,4(1-\cos\theta_\ell)\sin\theta_\ell\sin\theta_{\rm V}\;A\Re\left(e^{-i(\chi+\delta)}{\rm B}_{K^{*0}}\right)H_-H_0 \qquad \text{(3-c)}$$

Only the first term (3-a), $8\cos\theta_{\rm V}\sin^2\theta_\ell A\Re\left(e^{-i\delta}{\rm B}_{K^{*0}}\right)H_0^2$, will be present if one integrates over the acoplanarity variable χ. Since our acceptance is very uniform in χ, we will primarily observe the effects of 3-a when we average over χ. We will begin by studying the acoplanarity-averaged asymmetry distributions before turning attention to the two acoplanarity dependent terms: Eqn. 3-b and 3-c.

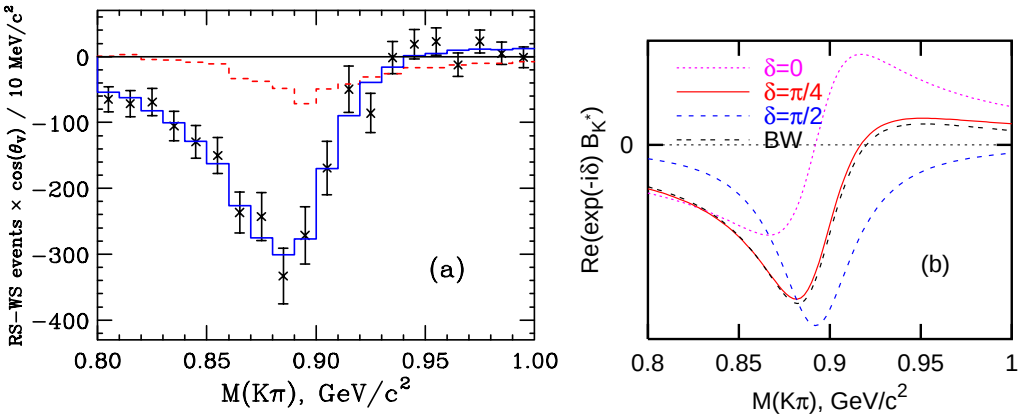

Fig. 4. Asymmetry distribution in $K\pi$ invariant mass. (a) The dashed line represents our Monte Carlo simulation with no interfering s-wave amplitude. The experimental data are the points with error bars. The solid line is the Monte Carlo with an s-wave amplitude of approximately 0.36 $(\text{GeV})^{-1}$, and a phase of $\frac{\pi}{4}$. Known charm backgrounds are simulated for both. (b) A plot of $\Re\left(e^{-i\delta}{\rm B}_{K^{*0}}\right)$ versus $m_{K\pi}$ for three choices of the phase δ. We also show an alternative modeling of the s-wave amplitude as a broad ($\Gamma = 0.4$ GeV/c^2) resonance with a mass of 1.1 GeV/c^2. We have put the broad, s-wave resonance in with a real phase relative to the K^{*0} Breit-Wigner, as one might expect given the presumed absence of final state interactions in semileptonic decay. This resonance solution is not unique.

The previously mentioned, weighted $m_{K\pi}$ distribution is shown in Figure 4. The shape of the $\cos\theta_{\rm V}$ term versus $m_{K\pi}$ is a strong function of the interfering s-wave amplitude phase δ. Because acceptance and resolution corrections are small, the phase can be informally determined from the $m_{K\pi}$ dependence expected from the interference of this phase with the phase variation expected for a Breit-Wigner, $\Re\left(e^{-i\delta}{\rm B}_{K^{*0}}\right)$. Figure 4(a) demonstrates that the $\cos\theta_{\rm V}$ weighted distribution in data is consistent with a constant s-wave amplitude of the form $0.36\ \exp(i\pi/4)\ (\text{GeV})^{-1}$. The magnitude of this amplitude is the value required to match the total asymmetry in data over the interval $0.8 < m_{K\pi} < 0.9$ GeV/c^2. In the discussion to follow, the s-wave amplitude will be fixed to this value.

We next turn to a discussion of the dependence of the acoplanarity-averaged linear $\cos\theta_{\rm V}$ term on other kinematic variables. Figure 5 compares the observed $\cos\theta_{\rm V}$ weighted distribution as a function of $\cos\theta_\ell$ to that expected in our model using our constant s-wave amplitude of 0.36 $\exp(i\pi/4)$ $(\mathrm{GeV})^{-1}$. We show the distributions for $m_{K\pi}$ both above and below 0.9 GeV/c^2.

In the context of our model, the acoplanarity-averaged, linear $\cos\theta_{\rm V}$ term should be of the form: $8\cos\theta_{\rm V}\sin^2\theta_\ell A\Re\left(e^{-i\delta}\mathrm{B}_{K^{*0}}\right)H_0^2$ and is proportional to $1-\cos^2\theta_\ell$. This parabolic dependence is quite evident in the weighted histogram shown in Figure 5 for those events with $m_{K\pi} < 0.9$ GeV/c^2 where the forward-backward asymmetry is the largest.

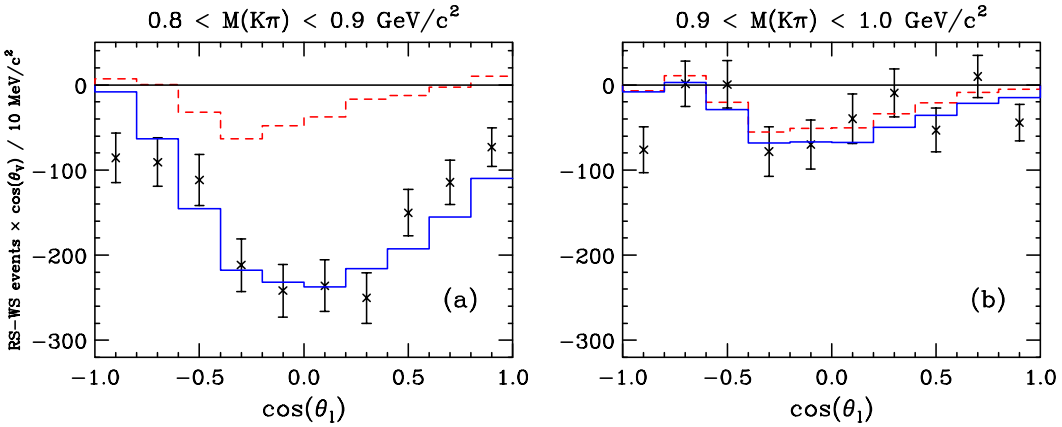

Fig. 5. Asymmetry distribution in $\cos\theta_\ell$ below (a) and above (b) the K^{*0} pole. The dashed line represents our Monte Carlo simulation with no interfering s-wave amplitude. The solid line is the Monte Carlo with an s-wave amplitude of approximately 0.36 $(\mathrm{GeV})^{-1}$, and a phase of $\frac{\pi}{4}$. We expect the acoplanarity-averaged interference to be proportional to $1-\cos^2\theta_\ell$, and to appear predominantly below the pole. Because the $\cos\theta_{\rm V}$ coefficient is negative, the weighted distribution appears inverted. The model with the s-wave amplitude is in good agreement with the data.

As a final test of the acoplanarity-averaged interference term, we examine the q^2 dependence of the linear $\cos\theta_{\rm V}$ coefficient. In our model, this coefficient should be proportional to $K\ q^2\ H_0^2(q^2)$. Figure 6 compares the $\cos\theta_{\rm V}$ weighted q^2 distribution to the data with and without the additional s-wave amplitude of 0.36 $\exp(i\pi/4)$ $(\mathrm{GeV})^{-1}$.

Eqn. 3-b and 3-c produce an s-wave interference term with sinusoidal variation in χ and are proportional to $\sin\theta_{\rm V}$. In the absence of the s-wave amplitude, all acoplanarity dependences either involve $\cos(2\chi)$ or are odd functions of $\cos\theta_{\rm V}$. The fact that (with the known form factors) the H_- term (Eqn. 3-c) dominates over the H_+ term has guided us in the construction of a weight to study the acoplanarity dependence of the s-wave interference. We weighted the acoplanarity distributions by weights of the form $\sin(\chi+\delta)$ and $\cos(\chi+\delta)$ where $\delta = \pi/4$ (the phase of s-wave amplitude in our model). We also multiplied these weights by $+1$ for right-sign events and -1 for wrong-sign events to subtract away the bulk of the non-charm background. For reasonably uniform

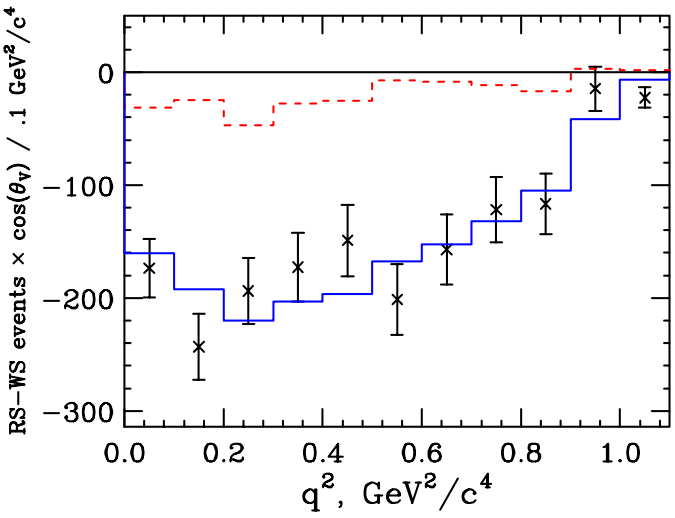

Fig. 6. Asymmetry as a function of q^2. The solid curve is our Monte Carlo including an interfering s-wave amplitude of 0.36 $\exp(i\pi/4)$ $(\mathrm{GeV})^{-1}$. The dashed curve has no interfering s-wave amplitude. Both Monte Carlo simulations include known charm backgrounds. The rightmost bin also includes those few events where $q^2 > 1.1(\mathrm{GeV}/c^2)^2$. The model with the s-wave amplitude is in good agreement with the data.

acceptance, these weights should average to zero for any constant or $\cos(2\chi)$ terms or any of the $\cos\theta_V \cos\chi$ terms present without s-wave interference.

Because the H_- term (Eqn. 3-c) dominates over the H_+ term, by offsetting the phase of the weight by the phase of our s-wave amplitude, we have arranged things such that the $\cos(\chi+\delta)$ weighted distribution should be proportional to $\Re(\mathrm{B}_{K^{*0}})$ (an odd function of $m_{K\pi}$-m_0) and the $\sin(\chi+\delta)$ weighted distribution should be proportional to $\Im(\mathrm{B}_{K^{*0}})$ (an even function of $m_{K\pi}$-m_0). These expectations are essentially borne out in the weighted plots shown in Figure 7.

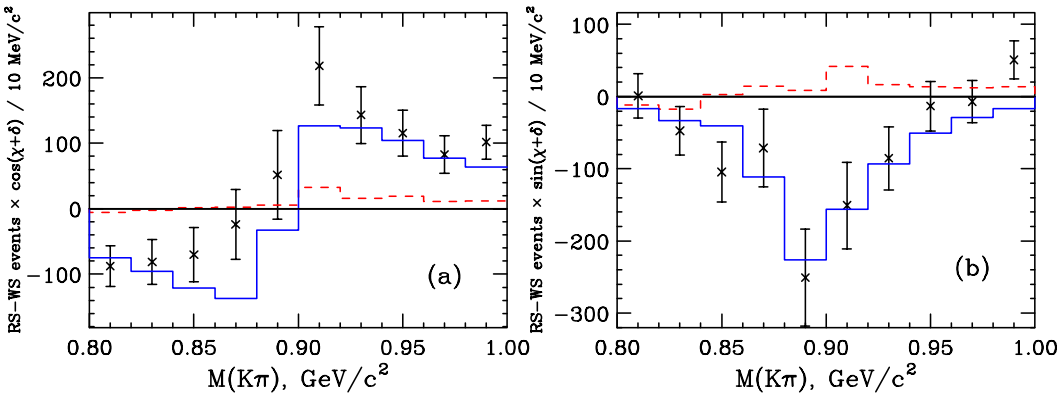

Fig. 7. Test of acoplanarity interference terms. Plot (a) uses the $\cos(\chi+\delta)$ and is expected to be proportional to the real part of a $\mathrm{B}_{K^{*0}}$ amplitude; while the plot (b) uses the $\sin(\chi+\delta)$ weighting and is expected to be proportional to the imaginary part of a $\mathrm{B}_{K^{*0}}$ amplitude. In both figures, the solid histogram is our Monte Carlo including the 0.36 $\exp(i\pi/4)$ $(\mathrm{GeV})^{-1}$ term; while in the dashed histogram there is no s-wave amplitude.

The presence of s-wave interference creates an interesting new complication in the conventions concerning the definition of the acoplanarity variable χ. Our conventions are guided by CP symmetry considerations. We define the sense of the acoplanarity variable via a cross product expression of the form: $(\vec{P}_\mu \times \vec{P}_\nu) \times (\vec{P}_K \times \vec{P}_\pi) \cdot \vec{P}_{K\pi}$ where all momenta vectors are in the D^+ rest frame. Since our χ convention involves five momenta vectors, we believe that as one goes from $D^+ \to D^-$ one must change $\chi \to -\chi$ in Eqn. 1. In the absence of the interference, there is no need to consider the sign conventions on χ since the decay distribution involves only cosines of χ or 2χ.

This point is made graphically by Figure 8 which compares the observed wrong-sign subtracted acoplanarity distribution for the D^+ and D^-. These distributions are quite consistent once the sign convention is properly reversed for the D^- relative to the D^+, indicating no evidence for CP violation in these decays.

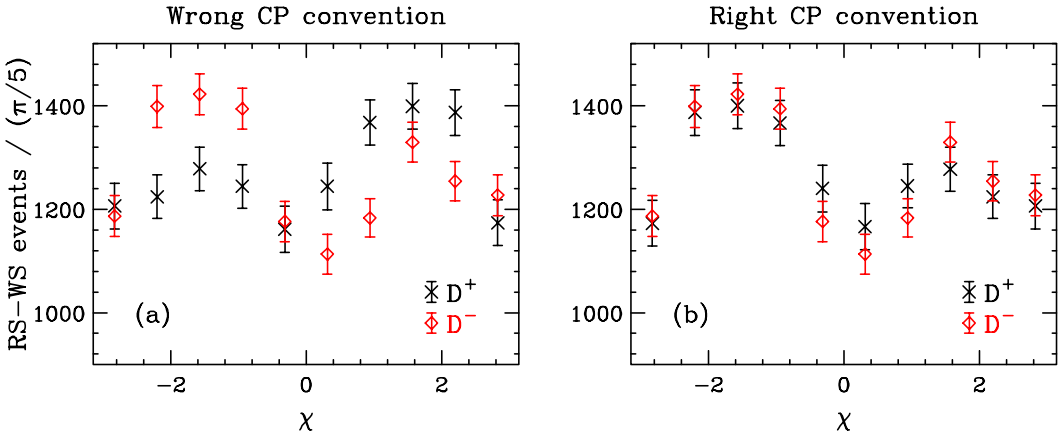

Fig. 8. The wrong-sign subtracted acoplanarity distribution separated by charm. The "x" points are for the D^+ while the "diamond" points are for the D^-. (a) compares the distributions without the required change in the χ convention as discussed above. (b) compares the distributions with the correct χ sign convention change.

We have presented compelling evidence for the existence of a coherent $K^-\pi^+$ s-wave contribution to $D^+ \to K^-\pi^+\mu^+\nu$. It has been assumed in all previous experimental analyses that this decay was strongly dominated by the process $D^+ \to \overline{K}^{*0}\mu^+\nu$. The previously unobserved, s-wave contribution is modeled as a constant amplitude of the approximate value $0.36\ \exp(i\pi/4)\ (\mathrm{GeV})^{-1}$. Its strength, 0.36, is roughly 7% of the $\overline{K}^{*0}$ Breit-Wigner amplitude at the pole mass in the term that couples to H_0 in Eqn. 1. The effect of this new interference is very noticeable in our data and creates a ≈15% forward-backward asymmetry in the variable $\cos\theta_V$ for $D^+ \to \overline{K}^{*0}\mu^+\nu$ events with $m_{K\pi}$ below the $\overline{K}^{*0}$ pole.

Although such an interference effect has been discussed in the phenomenological literature [6], there has been no discussion of it (to our knowledge) in the experimental literature. How could such a large effect have gone unnoticed in

the past? We believe one answer is that an amplitude of this strength and form creates a very minor modulation to the $m_{K\pi}$ mass spectrum as shown in Figure 9. Another reason is that this effect is much more evident when one divides the data above and below the $\overline{K}^{*0}$ pole as we have done. We were unable to find evidence that this particular split was studied in previously published data. Finally, the FOCUS data set has significantly more clean $D^+ \to K^-\pi^+\mu^+\nu$ events than previously published data.

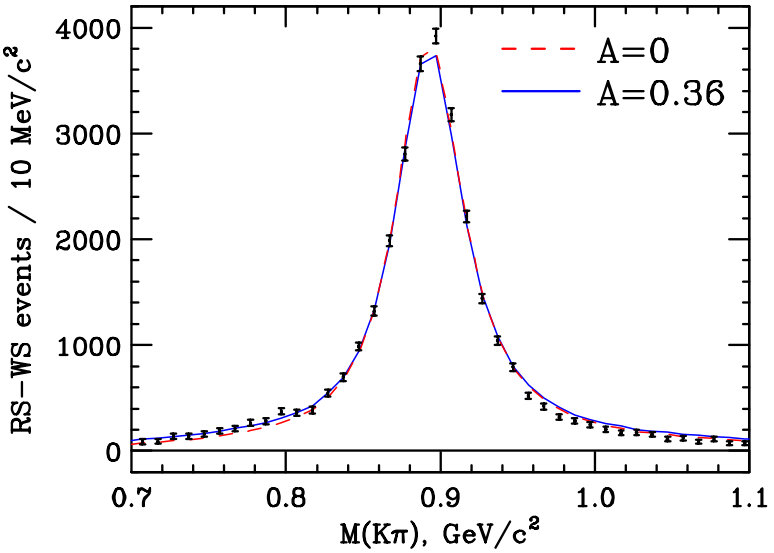

Fig. 9. We show the wrong-sign subtracted $m_{K\pi}$ distribution in data (points with error bars) and in two Monte Carlo simulations. The solid simulation includes the s-wave amplitude 0.36 $\exp(i\pi/4)$ $(\mathrm{GeV})^{-1}$; while the dashed simulation neglects it. The known charm backgrounds are included in both cases. Only a small modulation is observed primarily in the tails due to the inclusion of the new amplitude.

We wish to acknowledge the assistance of the staffs of Fermi National Accelerator Laboratory, the INFN of Italy, and the physics departments of the collaborating institutions. This research was supported in part by the U. S. National Science Foundation, the U. S. Department of Energy, the Italian Istituto Nazionale di Fisica Nucleare and Ministero dell'Università e della Ricerca Scientifica e Tecnologica, the Brazilian Conselho Nacional de Desenvolvimento Científico e Tecnológico, CONACyT-México, the Korean Ministry of Education, and the Korea Research Foundation.

References

[1] P.L. Frabetti et al., Phys. Lett. B **307**, 262 (1993); M. Adamocivh et al., Phys. Lett. B **268**, 142 (1991)

[2] Particle Data Group, J. Bartels et al., Eur. Phys. J. C**15** (2000) 1.

[3] See for example, J. M. Link et al., Phys.Lett.B485:62-70,2000 and references therein.

[4] J. M. Link et al., FERMILAB-Pub-01/243-E, hep-ex/0108011, to be published in Nucl. Instrum. Methods Phys. Res., Sect. A.

[5] J.G. Korner and G.A. Schuler, Z. Phys. C 46 (1990) 93.

[6] B. Bajc, S. Fajfer, R.J. Oakes, T.N. Pham, Phys. Rev. D **58** (1998) 054009.